Photoelectrochemical characterization of squaraine-sensitized nickel oxide cathodes deposited via screen-printing for p-type dye-sensitized solar cells

Photoelectrochemical characterization of squaraine-sensitized nickel oxide cathodes deposited via screen-printing for *p*-type dye-sensitized solar cells

Gaia Naponiello[a], Iole Venditti[a], Valerio Zardetto[b], Davide Saccone[c], Aldo Di Carlo[b], Ilaria Fratoddi[a,d], Claudia Barolo[c], Danilo Dini[a*]

[a] Department of Chemistry, Sapienza University of Rome P.le A. Moro 5, 00185 Rome, Italy

[b] Centre for Hybrid and Organic Solar Energy, Department of Electronic Engineering, University of Rome - Tor Vergata, via del Politecnico 1, 00133 Rome, Italy

[c] Department of Chemistry and NIS, Interdepartmental Centre of Excellence, University of Torino, via Pietro Giuria 7, I-10125 Torino, Italy

[d] Center for Nanotechnology for Engineering (CNIS), Sapienza University of Rome P.le A. Moro 5, 00185 Rome, Italy

*e-mail: danilo.dini@uniroma1.it

Abstract

In the present paper we report on the employment of the screen-printing method for the deposition of nickel oxide (NiO_x) layers when preformed nanoparticles of the metal oxide (diameter < 50 nm) constitute the precursors in the paste. The applicative purpose of this study is the deposition of mesoporous NiO_x electrodes in the configuration of thin films (thickness, $l \leq 4$ μm) for the realization of *p*-type dye-sensitized solar cells (*p*-DSCs). Three different squaraine-based dyes (here indicated with VG1C8, VG10C8 and DS2/35), have been used for the first time as sensitizers of a *p*-type DSC electrode. VG1C8 and VG10C8 present two carboxylic groups as anchoring moieties, whereas DS2/35 sensitizer possesses four acidic anchoring groups. All three squaraines are symmetrical and differ mainly for the extent of electronic conjugation. The colorant erythrosine b (ERY B) was taken as commercial benchmark for the comparison of the different dye-sensitizers. The influence of the conditions of NiO_x sensitization and of NiO_x surface pre-treatment on the photoelectrochemical performance of the corresponding p-DSCs have been analyzed. The highest overall conversion efficiency achieved within this set of organic colorants was 0.025 % with VG1C8 and VG10C8 as colorants when NiO_x surface was pre-treated with alkali. The alkaline pre-treatment of the NiO surface led to the highest efficiencies of the incident photon-to-current conversion ($IPCE_{MAX}$ = 11 % at about 390 nm) for the three squaraines here considered in correspondence of the wavelength of their maximum absorption. The prolongation of the sensitization time of NiO_x cathodes up to 16 hours leads to a general increase of the open circuit voltage in the corresponding *p*-DSCs.

Keywords: nickel oxide, *p*-type semiconductor, DSC, screen-printing, nanostructured materials, squaraine, organic sensitizer

Introduction

In the context of solar energy conversion the breakthrough represented by dye-sensitized solar cells (DSCs) or Grätzel's cells [1] as low cost devices alternative to p-n junctions which are capable of converting solar energy into electrical energy with reproducible efficiencies larger than 10 %,[2-5] opened a new direction of research to the scientists involved in the study of photo-electrochemical devices.[6] Beside electrochemists, the competencies required to develop increasingly efficient DSCs have to comprise inorganic and organic synthetic chemists, material scientists, solid-state physicists, optical and electrical engineers among others. The working principle of a DSC was first laid by Gerischer and Tributsch in the late sixties.[7] They reported charge injection into a wide bandgap semiconductor can be photoinduced indirectly by radiations with energy lower than the semiconductor bandgap[8] provided that a dye-sensitizer with opportune positioning of its frontier energy level modifies the semiconductor surface, and affords electron (or hole) tunneling into the semiconducting substrate upon photo-excitation.[9] The practical realization of photoelectrochemical cells based on the charge-transfer process actuated by immobilized photoexcited dyes relies on the fact that a dye brought in an electronically excited state is more prone to accept electrons as well as to release electrons with respect to its ground state.[10] Such a dual behavior implies that dye photoexcitation occurring at a sensitized semiconductor electrode increases the reducing power of the excited dye towards electron acceptors as well as the oxidizing power of the excited dye towards electron donors. The successive introduction of the characteristic of nanocrystallinity in semiconducting materials [11] rendered possible the absorption of a great number of dye-sensitizer molecules per unit area by virtue of the large electrode surface area[12] thus paving the way to the realization of much more efficient DSCs from early nineties on.[13] In the framework of photoelectrochemical DSC [14] the electron acceptors are represented by the oxidized form of a redox shuttle in the electrolyte,[15] or a *n*-type semiconductor substrate,[16] whereas the reduced form of a redox shuttle[17] and a *p*-type semiconductor substrate[18] constitute the electron donors that interact with the photoexcited dye-sensitizer of a DSC. Insofar the most important achievements on DSCs come from photoelectrochemical cells that utilize sensitized *n*-type semiconductors as photoactive electrode, namely TiO_2[19] and, at a lesser extent, ZnO,[20,21] whereas sensitized *p*-type electrodes have played a relatively marginal role.[22] The interest towards the research on *p*-type materials for DSCs purposes received a considerable input from the concept of tandem DSC in which a photoactive anode is combined with a photoactive cathode to provide a higher open circuit voltage and a larger theoretical efficiency with respect to the DSCs with single photoactive layer.[23,24] The major strength of the tandem device is related to the possibility of using two different dyes at the two semiconductor electrodes, which have complementary absorption features. This would allow the photoelectrochemical sensitization of both electrodes over a broader spectrum with respect to a DSC with single photoactive layer. The

most critical issue of a tandem DCS is represented by the lack of matching between the photocurrent densities of *n*-type and *p*-type sensitized electrodes, which prevents the realization of tandem DSCs as efficient as a *n*-type device. Because of that, it appears a quite stringent task to ameliorate the performance of *p*-type electrodes for DSCs. With NiO photocathodes the most important results have been achieved when P1[25-28] and PMI-6T-TPA[29] were the sensitizers. The present contribution focuses on the development of NiO cathodes in the configuration of thin films ($l \leq 4$ μm) with competitive photoelectrochemical performance in *p*-DSCs when the metal oxide films are deposited via screen printing method.[30] The novel aspect of our preparative approach consists in the insertion of preformed of NiO nanoparticles in the screen-printing paste. This is somewhat different to the preparative methods based on sol-gel chemistry so far used for the deposition of nanoporous NiO for *p*-type DSCs.[31-33] These methods of preparation involve traditionally the employment of two types of precursors: i) one for the formation of the metal oxide itself;[34] ii) one acting as binder/swelling agent for the formation of the mesoporous open morphology. In our approach only the precursors of the second type have been used while the first type of precursor has been replaced directly with metal oxide nanoparticles with proper diameter (less than 60 nm) in the screen-printing paste. The advantage of such a procedure is the generally lower temperature of processing (≤ 400-450 °C) with respect to sol-gel method (above 500 °C).[35,36] With the presence of nanoparticulated NiO in the starting paste the heat is used only to sinter the pre-existing metal oxide nanoparticles [37] but not for the activation of the chemical reactions that lead to the formation of the metal oxide. At the adopted operative temperature of sintering the binder is completely combusted and removed as a volatile product of thermolysis from the oxide layer. [34] The resulting oxide has generally non stoichiometric features and is better described by the generic formula NiO_x. Another general advantage of the screen-printing method of deposition is the attainment of uniform and adherent thick layers of mesoporous metal oxide deposits (up to 20 μm), which are crack-free and do not peel off from the substrate under ordinary conditions of transport and manipulation.[30] For the sensitization of the nanoporous NiO_x cathodes prepared via screen-printing method we have considered the series of organic dyes based on the squaraines of **Figure 1**.[38] This class of dyes has been previously used with success for the sensitization of NiO_x,[39-42] and represents a crucial node in the perspective of assembling a tandem device.[23,24] This is because the squaraines possess absorption properties which are complementary to those of the traditional organometallic [43]and organic dyes [44] used for the sensitization of *n*-type DSCs (with TiO_2 or ZnO working electrodes). The choice of the three symmetric squaraines VG1C8, VG10C8 and DS2/35 (**Figure 1**) with their red-shifted absorption [38] with respect to the more largely used organic sensitizers of NiO cathodes [23,28,29] was motivated by the easiness of their preparation and the lower costs of purification with respect to their unsymmetrical analogues.[45] The successful employment of the squaraines VG1C8 [45] and

VG10C8[46] as sensitizers of *n*-type DSCs has been previously demonstrated when nanoporous TiO_2 was the electrode.[47] In the present paper we intend to proof the concept of *p*-type NiO sensitization with the same series of squaraines of **Figure 1**. The use of DS2/35 dye as sensitizer is reported here for the first time. Colorant ERY B [23,37,48] has been chosen as commercial benchmark dye-sensitizer for the confronted evaluation of the photolectrochemical performances of the *p*-DSCs based on the differently sensitized screen-printed cathodes.

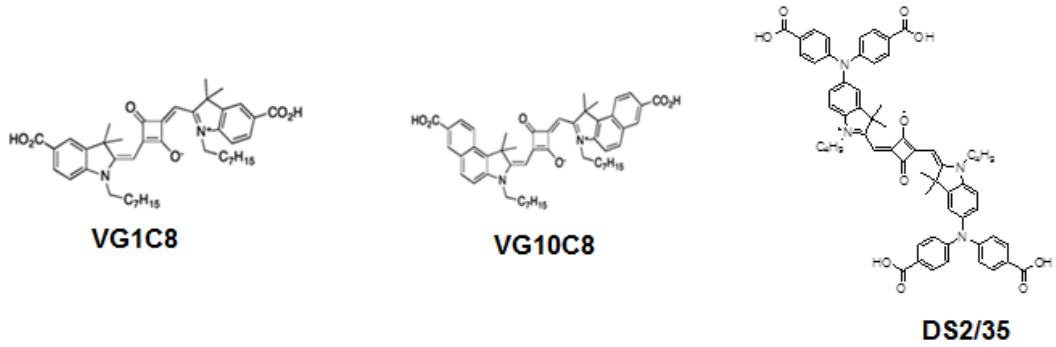

Figure 1. Structure of the three squaraines VG1C8, VG10C8 and DS2/35 here utilized as organic sensitizers of screen-printed NiO cathodes for *p*-DSCs.

Experimental section

Preparation of the NiO_x paste

The preparation of the NiO_x paste for the successive screen-printing deposition is realized through the multistep procedure presented in Table 1. This paste preparation procedure is a slightly modified version of the one reported by Ito *et al.* for the preparation of the TiO_2 paste to be utilized in screen-printing procedures.[30] All chemicals were purchased from Fluka or Sigma-Aldrich at the highest degree of purity available and were used without any further purification.

Anhydrous terpineol was added as an mixture of enantiomers. Grinding of the various mixtures obtained at the different steps (Table 1) was effectuated at ambient conditions in a mortar having a diameter of 20 cm. Stirring was conducted with a 4 cm long magnetic stirrer at rotation speed of 300 rpm. The ultrasonic homogenization was performed with a Ti-horn-equipped sonicator (Vibra cell 72408 from Bioblock scientific). The final paste had the appearance of a viscous slurry and was stable up to six months.

Screen-printing deposition of NiO_x coatings

The NiO_x paste obtained from the multistep procedure of Table 1 was spread over FTO covered glass panels [from Solaronix (item no. TCO22-7)]. Prior to paste spreading, the substrates of glass/FTO covered were cleaned by an ultrasonic bath in acetone for 10 min and subsequently in ethanol for 10 min. After the two-step washing procedure the FTO/glass panels were dried in air.

The paste was deposited via screen printing through a 90.48 T mesh screen on dried FTO/glass panels. After a step of moderate heating at 80° C for 15 min, the screen-printed slurry of NiO nanoparticles was sintered at 450°C for 6 h. After sintering the resulting mesoporous films of NiO were cooled down to ambient temperature. The thickness, l, of the NiO_x film (thickness range: $2 \leq l \leq 4$ μm) was determined with a Dektak 150®profilometer from Veeco. The imaging of the surface morphology of mesoporous NiO_x (**Figure 2**) was realized with an Auriga Zeiss instrument.

Step 1	6g of NiO nanopowder are grinded with 1mL of glacial acetic acid for 5 min (final volume of mixture: 1 mL)
Step 2	Addition of 1mL of H_2O to the mixture obtained after Step 1 and grinding for 1 min. This succession is repeated 5 times (final volume of mixture: 6 mL)
Step 3	Addition of 1mL of ethanol to the mixture of Step 2 and grinding for 1 min. This succession is repeated 15 times (final volume of the mixture: 21 mL)
Step 4	Addition of 2.5mL of ethanol to the mixture of Step 3. This succession is repeated 6 times (final volume of the mixture: 36 mL)
Step 5	Transfer of the paste of Step 4 to a beaker using 100 mL of ethanol (final volume of the mixture: 136 mL)
Step 6	The mixture of Step 5 is stirred 1 min, successively sonicated for 2 min and finally stirred again for 1 min
Step 7	Addition of terpineol (20 g)
Step 8	The mixture of Step 7 is stirred 1 min, successively sonicated for 2 min and finally stirred again for 1 min
Step 9	Addition of a solution of ethyl cellulose to the mixture of Step 8. The added solution is formed by adding 3 g of ethyl cellulose in 30g of a 10% v/v solution of ethanol in aqueous solvent
Step 10	The mixture of Step 9 is stirred 1 min, successively sonicated for 2 min and finally stirred again for 1 min. This succession of 4 min is repeated 3 times
Step 11	Slow evaporation of the volatile components of the resulting mixture: The mixture of Step 10 is placed on hot plate at 50°C for 9 hours. After then the NiO nanoparticles paste is cooled down to ambient temperature and ready for being utilized in the screen-printing mode of deposition

Table 1. Procedure for the preparation of the nickel oxide paste for screen-printing

Electrochemical characterization of NiO_x coatings

The electrochemical properties of bare NiO_x films were analyzed with an Autolab PGSTAT12® potentiostat/galvanostat driven by the Autolab software Nova 1.9. Cyclic voltammograms were recorded using a three-electrode cell configuration: NiO_x substrates were employed as the working

electrodes; a platinum wire as the counter electrode and Ag/AgCl electrode as the reference. A solution of $LiClO_4$ (concentration: 0.2 M) in CH_3CN was used as electrolyte.

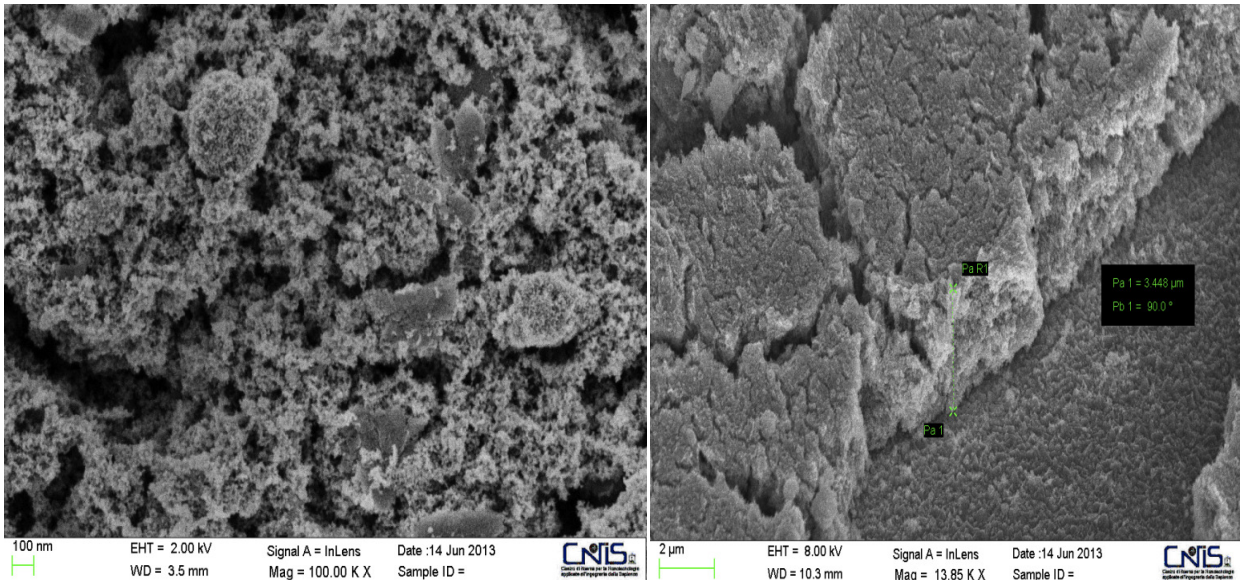

Figure 2. FE-SEM images showing (left) surface morphology and (right) cross-section of the mesoporous NiO_x electrode obtained via screen-printing.

Sensitization of NiO_x coatings

Screen printed photocathodes of NiO_x were dipped in a 0.1 mM dye-sensitizer solution with ethanol as solvent. Oxide samples were sensitized at room temperature with two different durations of immersion: 2 and 16 h. In a series of characterizations the NiO_x electrode was pre treated with alkali before sensitization. Alkali treatment of oxide surface consisted in the immersion of the as prepared NiO_x in a 0.1 M NaOH solution in water solvent. NiO_x was immersed for two hours in the aqueous solution of NaOH.

Synthesis of squaraines

The details of the synthesis of colorants VG1C8 and VG10C8 have been reported previously in refs.45 and 46, respectively. Dye DS2/35 (Figure 1) has been prepared according to Scheme 1.

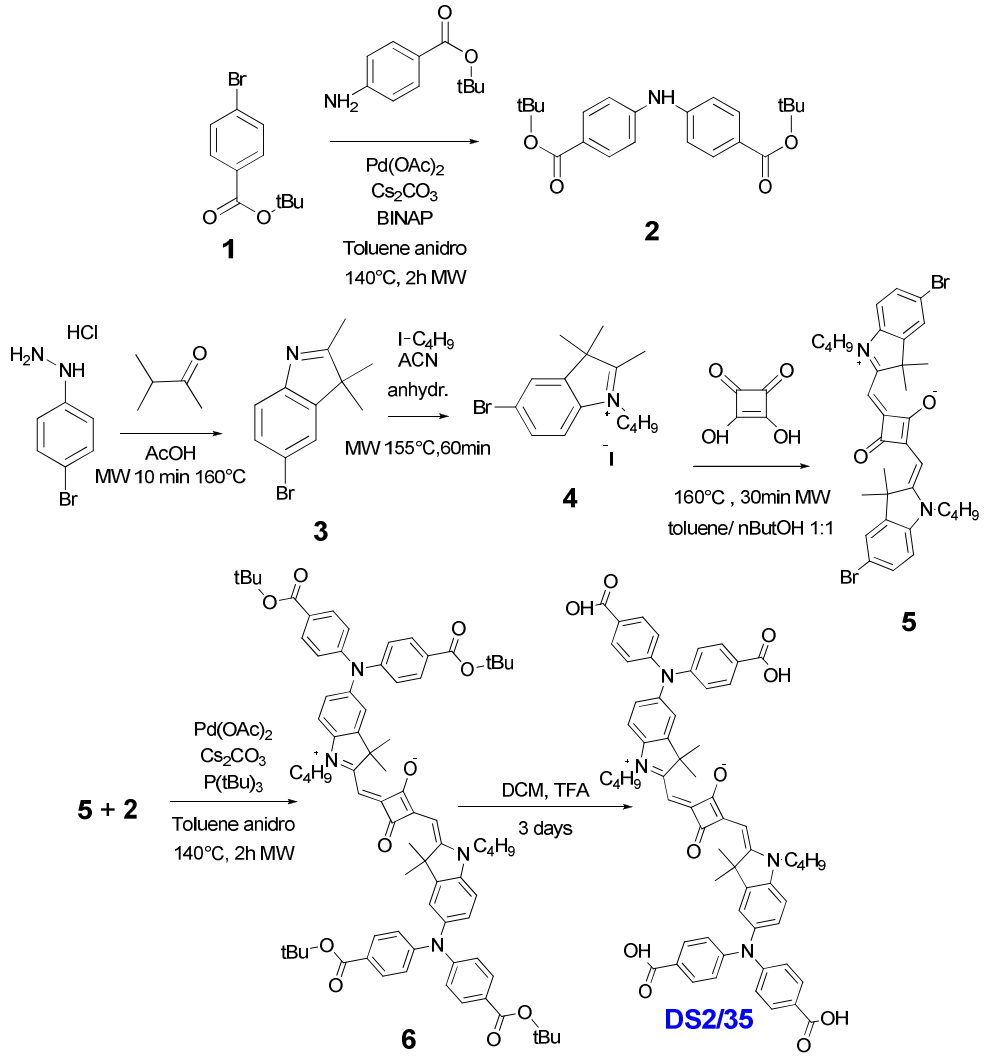

Scheme 1. Synthesis of dye-sensitizer DS2/35

For the synthesis of DS2/35 as described in Scheme 1, all reagents and solvents were either ACS reagent grade or HPLC/spectroscopy grade and were obtained from Sigma-Aldrich. Reagents were used without further purification. The microwave reactions were done with a Biotage® Initiator 2.5 Microwave Synthesizer. MPLC purification were obtainded with Biotage® Isolera or Biotage® SP1. Electro-spray ionization (ESI) experiments were conducted with a Thermo Finnigan Advantage Max Ion trap spectrometer in negative and positive ion acquiring mode. The sheath gas flow rate was set at 25 (arbitrary unit), auxiliary gas flow rate at 5 (arbitrary unit), spray voltage at 3.25 KV, capillary temperature at 270 °C, capillary voltage at 7 V, and tube lens offset at 60.00 V.

Nitrogen was used as sheath and auxiliary gases. HPLC analyses were performed on a Shimadzu HPLC 10-AVP series equipped with a photodiode array SPD-M 10 AVP as a detector using as solid phase Fusion column 4.6 mm * 250 mm with MeOH as liquid phase. ^{1}H NMR and 13C NMR spectra were recorded with a Bruker AM–200 spectrometer. The reported chemical shifts are relative to the signal of TMS. The details of the preparation and characterization of precursors **1**-**6** are given in the supplementary information (SI).

DSCs assembly and testing

Platinized counter electrodes were prepared by screen printing platinum paste Ch01 from Chimet through a 100T mesh screen onto FTO-coated glass. [49] Sensitized NiO_x photoelectrode and counter electrodes were assembled together in a sandwich configuration. A Bynel® thermoplastic polymer film was used as both spacer and sealant for the *p*-type DSCs. Finally, iodine/iodide HSE commercial liquid electrolyte (from Solaronix) was injected inside the cells by vacuum backfilling technique. The active area for all the samples was 0.25 cm^2. The experimental apparatus for the realization of the experiments under irradiation with solar simulator AM 1.5G (Intensity: 1000 W m^{-2}), i.e. JV curves, incident photon-to-current efficiency (IPCE) spectra, has been described in ref. 40. The photovoltaic performance of the cells was measured under a solar simulator Solar Test 1200 KHS. IPCE curves were recorded using a computer controlled set-up consisting of a Xe lamp (Mod. 70612, Newport) coupled to a monochromator (Cornerstone 130, from Newport), and a Keithley 2420 light-source meter.

Results and Discussion

Electrochemical properties of screen-printed NiO_x

Screen-printed NiO_x in non aqueous electrolyte presents a voltammogram characterized by the presence of two broad peaks of oxidation: one localized between 0.2 and 0.3 V *vs* Ag/AgCl and another with an ill defined shape between 0.6 and 1 V *vs* Ag/AgCl (**Figure 3**). Both present quasi reversibile features and refer to the following solid state oxidation processes of NiO_x:[50,51]

$$Ni^{(II)}_{1-y}Ni^{(III)}_{y}O_{1+y/2} + m\ X^- \rightarrow Ni^{(II)}_{1-y-m}Ni^{(III)}_{y+m}O_{1+y/2}(X)_m + m\ e^- \qquad \{1a\}$$

$$Ni^{(II)}_{1-y-m}Ni^{(III)}_{y+m}O_{1+y/2}(X)_m + n\ X^- \rightarrow Ni^{(II)}_{1-y-m}Ni^{(IV)}_{y+m+n}O_{1+y/2}(X)_{m+n} + n\ e^- \qquad \{1b\}$$

These mechanisms consider the uptake of anions (X^- in Eqs. 1) from the supporting electrolyte, which compensate the positive charge introduced in NiO_x upon oxidation. The charge compensating anions will be localized either on the surface of the metal oxide[50] or eventually within its structure.[52]

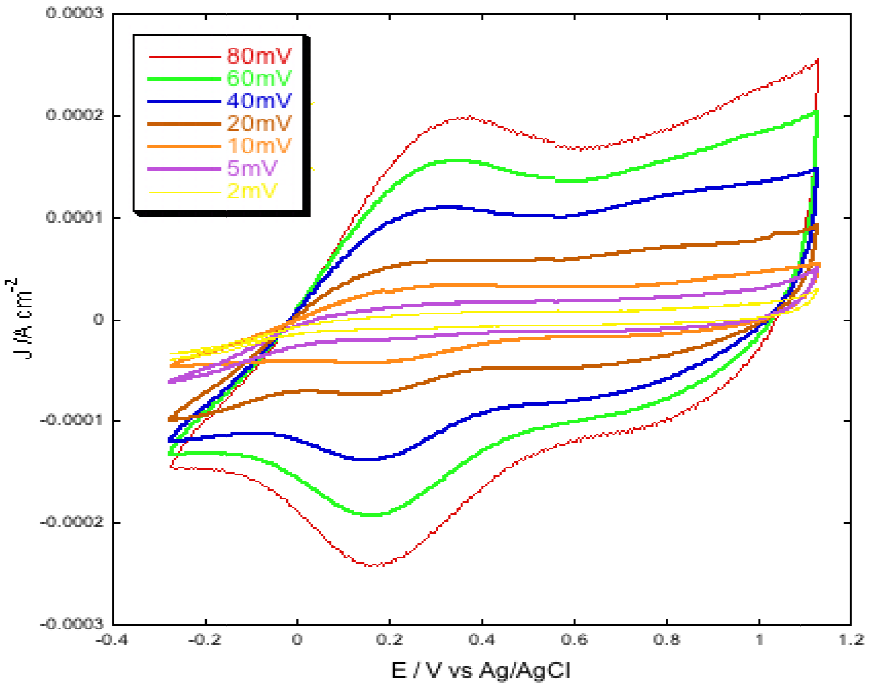

Figure 3. Voltammograms of bare NiO thin film electrode (thickness: 2 µm) prepared via the screen-printing method at different scan rates. Electrolyte: 0.2M $LiClO_4$ in acetonitrile**.**

The analysis of the scan rate dependence of the intensity of the current peaks shows a linear relationship between these two parameters. This is shown for the current peak associated to the process of Eq.1a and occurring at about 0.25 V *vs* Ag/AgCl (**Figure 4**).

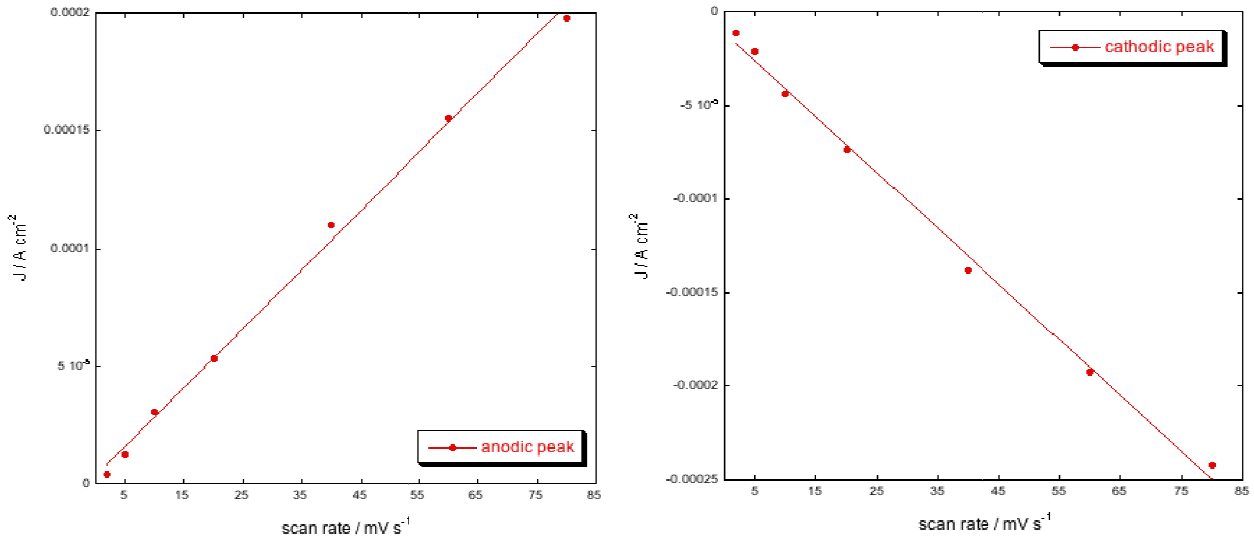

Figure 4. Linear dependence of the current peak centered at 0.25 V *vs* Ag/AgCl with scan rate (data taken from the voltammograms of **Figure 3**). Left: variation of the anodic current peak; right: variation of the cathodic current peak.

This finding is indicative of the occurrence of redox reactions that are kinetically controlled by a charge transfer process confined at the NiO/electrolyte interface.[53] Therefore, the NiO sample obtained via screen printing of preformed oxide nanoparticles displays the same type of electrochemical behavior of nanostructured NiO prepared via RDS[50] and via the sol-gel route.[51] When the voltammograms of screen-printed NiO_x films with different thickness are compared (**Figure 5**), we observe a direct proportionality between film thickness and amount of exchanged current. This finding recalls our previous observations on the voltammograms of CS [53] and RDS NiO_x samples [26,50] conducted for metal oxide samples with different thickness. We conclude that also mesoporous screen-printed NiO_x (**Figure 2**) presents electroactivity throughout the whole thickness and displays an effective electrical contact at the NiO_x/FTO interface.[54]

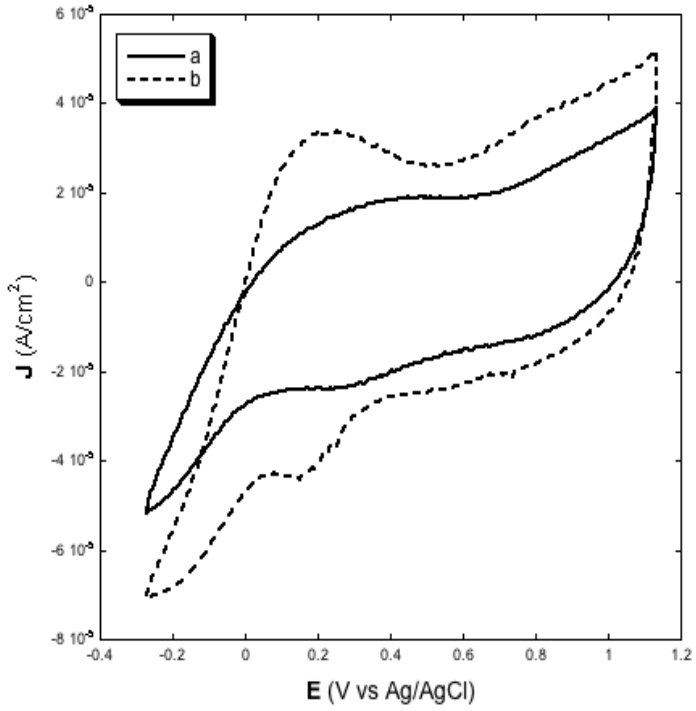

Figure 5. Effect of NiO_x film thickness (l) on the voltammogram recorded in non aqueous electrolyte (electrolyte composition as in **Figure 3**). Scan rate: 5 mV s^{-1}. Curve a(full line): l = 2 µm; curve b (dotted line): l = 4 µm.

Characterization of the p-DSC with screen-printed NiO_x cathodes

Screen-printed NiO_x cathodes with thickness 4 µm were sensitized with ERY B, VG1C8, VG10C8 and DS2/35 at two different durations of dipping: 2 h and 16 h. The corresponding transmission spectra of these series of electrodes are presented in **Figure 6**.

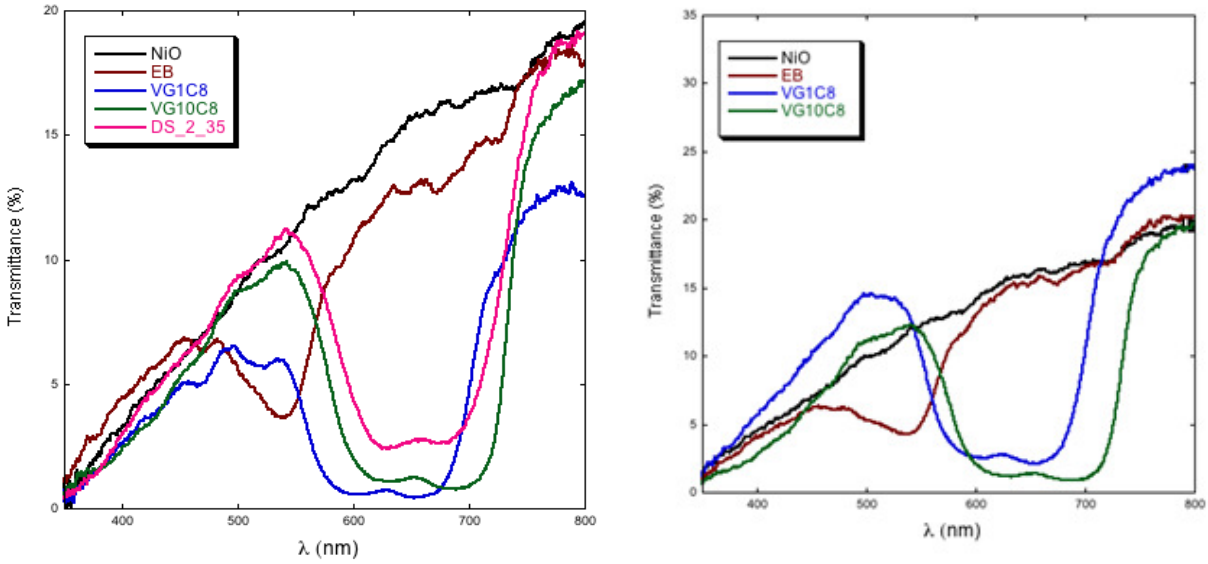

Figure 6. Transmission spectra of bare and sensitized screen-printed NiO_x (l = 4 µm) when sensitization lasts (left) 2 h and (right) 16 h. Transmission spectrum of DS2/35 sensitized NiO_x remains unchanged with the duration of sensitization and has not been reported in the right plot.

The effect of sensitization is particularly evident in the spectral range 470-730 nm with the squaraines decreasing the optical transmission of the sensitized screen-printed oxide at the largest wavelengths. Duration of sensitization with the selection of dye-sensitizer here considered does not seem to play a relevant role in the modification of the optical spectrum of the sensitized oxide. The *JV* characteristic curves of the corresponding *p*-DSCs are presented in **Figure 7**.

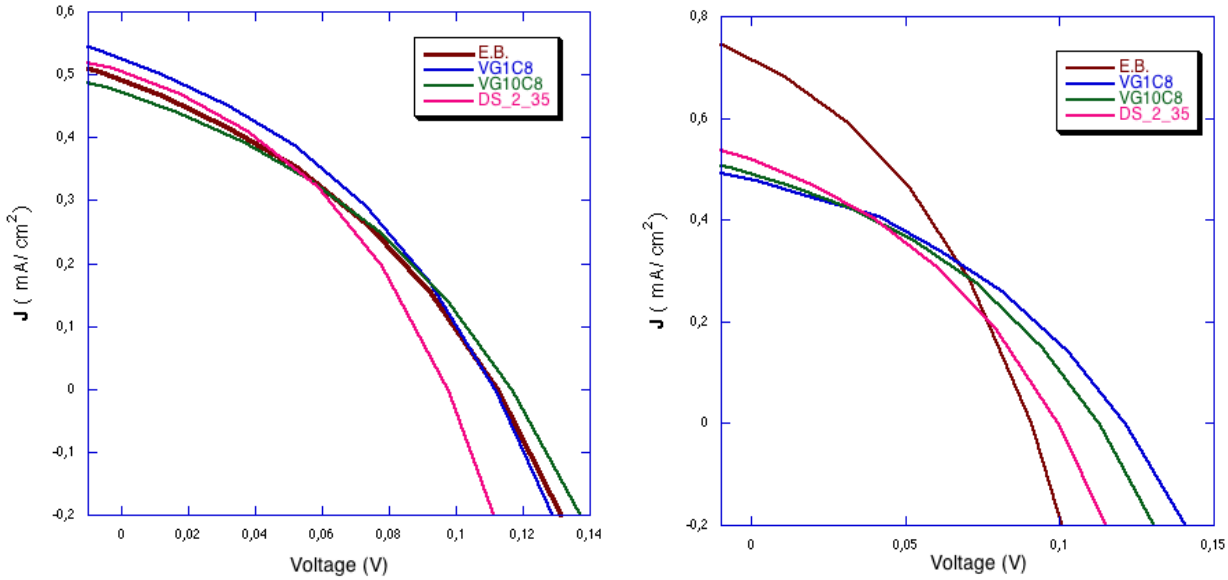

Figure 7. *JV* characteristic curves of the *p*-DSCs with sensitized screen-printed NiO_x cathodes (l = 4 µm) when sensitization lasts (left) 2 h and (right) 16 h.

The IPCE spectra associated with the characteristic curves of **Figure 7** are presented in **Figure 8**.

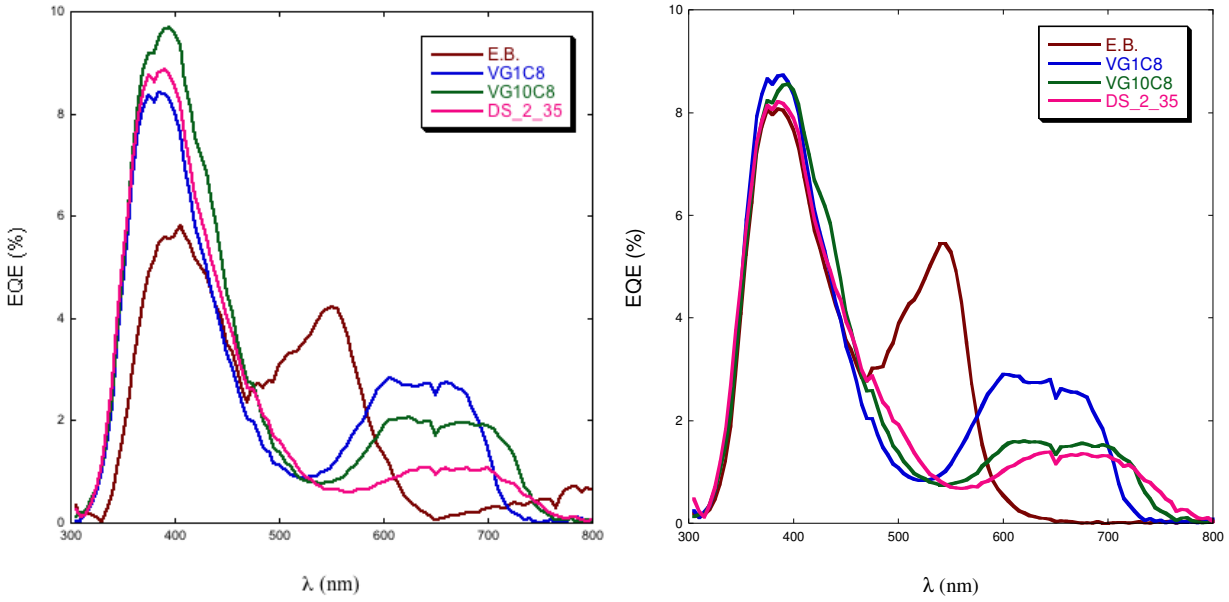

Figure 8. IPCE spectra of *p*-DSCs utilizing sensitized screen-printed NiO_x (l = 4 μm) when sensitization lasts (left) 2 h and (right) 16 h. EQE represents the external quantum efficiency.

Prolonged sensitization for 16 h has an evident beneficial effect only on the performance of the *p*-DSC with ERY B as sensitizer of the screen-printed NiO_x cathode (Tables 2 and 3). Overall efficiency increases from 0.019 % to 0.024 % on passing from 2 h to 16 h of sensitization due mainly to the increase of J_{SC} (0.480 mA cm^{-2} *vs* 0.697 mA cm^{-2}). When confronted with the overall efficiency of highly performing NiO_x cathodes sensitized with the same type of colorant ERY B (η = 0.045 %),[48] we observe generally lower values of η for the *p*-DSCs with screen-printed NiO_x electrodes. In case of NiO_x sensitization with squaraine-based molecules, the prolongation of the dipping time does not bring about any substantial improvement of the performance of the corresponding *p*-DSCs η being always comprised within the narrow range 0.019-0.021 % (Tables 2 and 3). From the IPCE spectra we can distinguish the photoelectrochemical contribution due to bare NiO_x within the wavelength range 300-480 nm,[40] from the photoeffect produced by the organic sensitizers at wavelengths larger than 500 nm (**Figure 8**).

Dye	Voc (mV)	Isc (mA)	Jsc (mA/cm2)	FF(%)	η (%)
Erythrosine B	112	0.120	0.480	35.7	0.019
DS2/35	98	0.123	0.494	39.1	0.019
VG1C8	112	0.128	0.515	36.9	0.021
VG10C8	117	0.116	0.465	35.5	0.019

Table 2. Parameters of the *p*-DSCs with screen-printed NiO_x (l = 4 μm) cathodes sensitized 2 h. Symbols V_{OC}, I_{SC}, J_{SC}, FF and η are for open circuit voltage, short circuit current, short circuit current density, fill factor and overall efficiency, respectively.

Dye	Voc (mV)	Isc (mA)	Jsc (mA/cm2)	FF(%)	η (%)
Erythrosine B	90	0.174	0.697	37.4	0.024
DS2/35	100	0.127	0.507	36.7	0.019
VG1C8	121	0.118	0.471	36.9	0.021
VG10C8	113	0.120	0.481	36.9	0.020

Table 3. Parameters of the *p*-DSCs with screen-printed NiO_x (l = 4 μm) cathodes sensitized 16 h.

We have also adopted an original approach within the framework of nickel oxide sensitization by modifying the anchoring properties of nanoporous NiO_x by means of the treatment of bare NiO_x surface with alkali. Prior to sensitization with the series of organic dyes here considered (**Figure 1**), screen-printed NiO_x was immersed for 2 h in an aqueous solution of NaOH (c_{NaOH} = 0.1 M). The aim of this alkali treatment is twofold: i) to neutralize possible acidic sites on the surface of pristine screen-printed NiO_x following its hydration in ambient conditions[50] [the presence of acidic surface sites would prevent the successive hydrolysis reaction of oxide sensitization via the carboxilic group(s) (anchoring moiety) of the dye sensitizer]; ii) to shift the frontier energy levels of the alkali treated metal oxide following the removal of surface protons.[55] The latter effect could have a favourable influence on the kinetics of hole photo-injection in the sensitized oxide as well as on the

matching between the frontier levels of NiO_x and photoexcited dye. The treatment with alkali does not seem to affect the optical spectrum of bare NiO_x (**Figure 9**) with respect to its pristine version (**Figure 6**) since both metal oxide versions present a featureless spectrum within the visible range and display comparable values of optical transmittance.

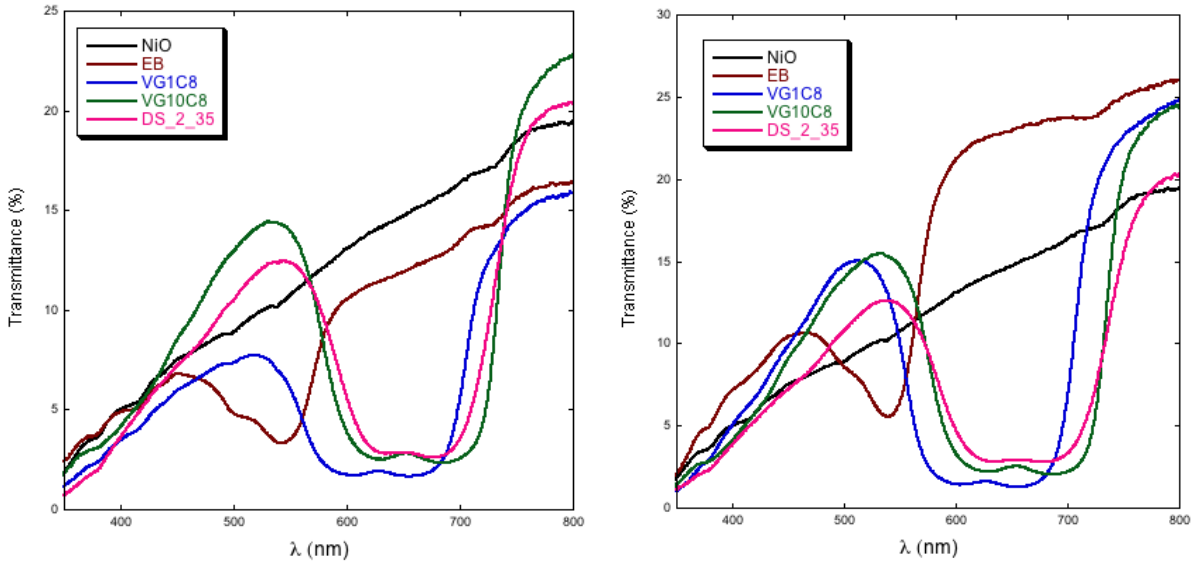

Figure 9. Comparison between the transmission spectrum of bare NiO_x (l = 4 μm) immersed in an alkali solution for two hours and the transmission spectra of the alkali treated NiO_x sensitized for (left) 2 h and (right) 16 h.

The *JV* curves of the *p*-DSC with alkali treated NiO_x photocathodes are presented in **Figure 10**. The prolongation of the sensitization time has a generally favourable effect on the short circuit current densities for those *p*-DSCs with alkali treated NiO_x cathodes sensitized with ERY B, VG1C8 and VG10C8 (Tables 4 and 5). On the contrary, the sensitization with DS2/35 gives better results when the dipping time of the alkali treated NiO_x in the tincture solution is shorter. The most noticeable increase of overall efficiency with the prolongation of the dipping time is observed for the *p*-DSC with VG10C8 as dye-sensitizer when screen-printed NiO_x is alkali treated. When the *p*-DSCs performances of the alkali treated NiO_x cathodes are compared with the corresponding ones utilizing untreated NiO_x, a general increase of overall efficiency is observed for the alkali treated cathodes if ERY B, VG1C8 and VG10C8 are the sensitizers. In this analysis the dye DS2/35 constitutes the sole exception since the optimized *p*-DSC cell performance with DS2/35-sensitized NiO_x is recorded when the mesoporous screen-printed electrode is not alkali treated and is dipped in the tinc-

ture solution for short times not exceeding 4 hours (Tables 2-5). This singular behaviour might be a consequence of the larger number of anchoring groups in DS2/35 with respect to the other squaraine-based dyes (four *vs* two, see **Figure 1**), which might affects the kinetics of sensitization as well as the geometry of the interaction between dye and oxide in the photoactivated process of charge transfer.

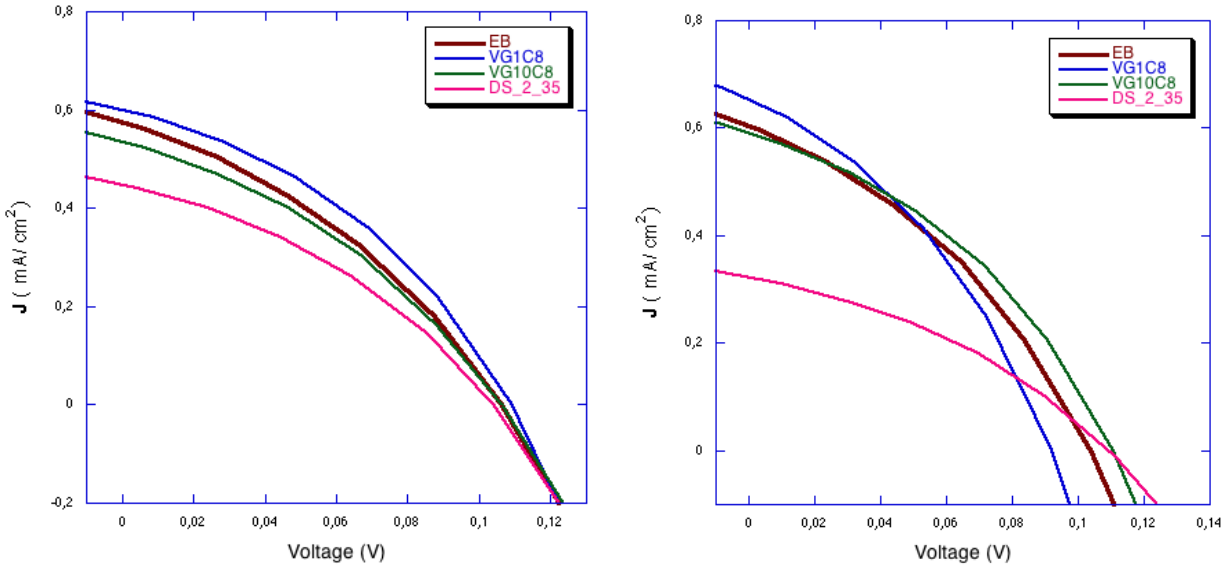

Figure 10. *JV* characteristic curves of alkali treated NiO_x (l = 4 µm) sensitized with ERY B, VG1C8, VG10C8 and DS2/35. Sensitization duration: (left) 2 h; (right) 16 h.

The IPCE spectra have been recorded for the *p*-DSCs with alkali treated electrodes when these were sensitized at two different dipping times (**Figure 11**). In the experimental conditions of IPCE curve determination the differences between the spectra of the *p*-DSCs with alkali treated electrodes are minimal and do not result strongly affected by the duration of dipping. Moreover, the duration of dipping does not influence the shape of the spectra thus indicating that the state of the anchored dye, i.e. if isolated or aggregated, does not change with the duration of sensitization in the adopted range of dipping time.

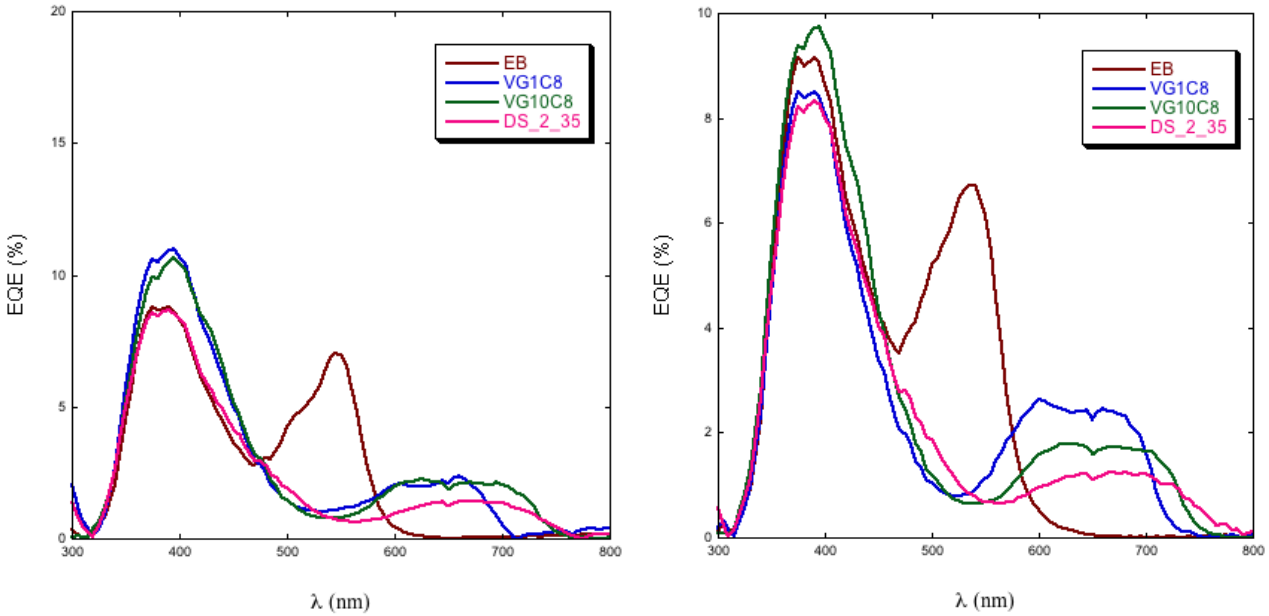

Figure 11. IPCE spectra of the *p*-DSCs utilizing alkali treated NiO_x (l = 4 μm) cathodes sensitized with ERY B, VG1C8, VG10C8 and DS2/35. Sensitization duration: (left) 2 h; (right) 16 h.

Dye	V_{oc} (mV)	i_{SC} (mA)	J_{SC} (mA cm^{-2})	*FF* (%)	η (%)
ERY B	126	0.063	0.251	36.5	0.022
DS2/35	124	0.055	0.218	36.9	0.017
VG1C8	119	0.084	0.335	40.5	0.024
VG10C8	127	0.059	0.238	36.2	0.020

Table 4. Parameters of the *p*-DSCs with alkali treated NiO_x (l = 4 μm) cathodes sensitized 2 h.

Dye	V_{oc} (mV)	i_{SC} (mA)	J_{SC} (mA cm^{-2})	*FF* (%)	η (%)
ERY B	109	0.090	0.360	37.0	0.022
DS2/35	130	0.035	0.140	36.6	0.013
VG1C8	112	0.087	0.355	37.3	0.022
VG10C8	130	0.071	0.288	38.8	**0.025**

Table 5. Parameters of the *p*-DSCs with alkali treated NiO_x (l = 4 μm) cathodes sensitized 16 h.

Conclusions

We have presented a novel method of preparation of mesoporous NiO_x thin films (thickness, $l \leq 4$ μm) for *p*-type dye-sensitized solar cells (*p*-DSCs) purposes based on the screen-printing technique. The innovative point consists in the direct utilization of preformed of NiO nanoparticles in the screen-printing paste, which requires relatively lower temperature of processing (≤ 400-450 °C). In this study we have considered for the first time three different squaraine-based dye-sensitizers (VG1C8, VG10C8 and DS2/35), which differed mainly for the extent of electronic conjugation. Erythrosine b was also utilized as dye benchmark for sensitizing NiO_x photocathodes. The best photoelectrochemical performances in terms of overall conversion efficiency have been obtained with the colorants VG1C8 and VG10C8. The influence of the conditions of NiO_x sensitization and of NiO_x surface pre-treatment on the photoelectrochemical performance of the corresponding *p*-DSCs were also analyzed. Higher efficiencies could be reached with the same squaraines VG1C8 and VG10C8 when the surface of NiO_x was pre-treated with alkali. The prolongation of the dipping time for the sensitization of screen-printed NiO_x cathodes has a favorable effect on the open circuit voltage of the corresponding *p*-DSCs. Further studies are in progress to optimize sintering conditions and modify the chemical composition of the paste with the aim of producing more efficient photoactive cathodes for *p*-DSCs when NiO_x thin films are deposited via screen-printing. Moreover, new colorants based on the squaraine skeleton are envisaged for the more effective sensitization of *p*-type NiO_x.

Acknowledgments

This research project was supported by Regione Lazio and CHOSE. The authors acknowledge the financial support of Ateneo Sapienza 2011/VG1-C26A11PKS2. This work was partially supported by the Dipartimento di Chimica, Sapienza Università di Roma through the *Supporting Research Initiative 2013*. C.B. gratefully acknowledges financial support by DSSCX project (PRIN 2010-2011, 20104XET32) from Ministero dell'Istruzione, dell'Università e della Ricerca and the University of Torino (Ricerca Locale ex-60%, Bando 2012).

References

1. B. O'Regan, M. Grätzel, Nature 353 (1991) 737

2. A. Yella, H.W. Lee, H.N. Tsao, C. Yi, A. Kumar Chandiran, M.K. Nazeeruddin, E.W.G. Diau, C.Y. Yeh, S.M. Zakeeruddin, M. Grätzel, Science 334 (2011) 629

3. Y.Q. Wang, B. Chen, W.J. Wu, X. Li, W.H. Zhu, H. Tian, Y.S. Xie, Angew. Chem. Int. Ed. 53 (2014) 10779

4. Y. Chiba, A. Islam, Y. Watanabe, R. Komiya, N. Koide, L. Han, Jpn. J. Appl. Phys. 45 (2006) L638

5. S. Mathew, A. Yella, P. Gao, R. Humphry-Baker, B.F.E. Curchod,N. Ashari-Astani, I. Tavernelli, U. Rothlisberger, M.K. Nazeeruddin, M. Grätzel, Nature Chem. 6 (2014) 242

6. J.M. Kroon, N. J. Bakker, H.J.P. Smit, P. Liska, K.R. Thampi, P. Wang, S.M. Zakeeruddin,M. Grätzel, A. Hinsch, S. Hore, U. Würfel, R. Sastrawan, J.R. Durrant, E. Palomares, H. Pettersson, T. Gruszecki, J. Walter, K. Skupien, G.E. Tulloch, Progr. Photovolt. Res. Appl. 15 (2007) 1

7. H. Gerischer, H. Tributsch, Electrochim. Acta 13 (1968) 1509

8. P. Liska, N. Vlachopoulos, M.K. Nazeeruddin, P. Comte, M. Grätzel, J.Am. Chem. Soc. 110 (1988) 3686

9. H. Gerischer, F. Willig, Topics Curr. Chem. 61 (1976) 31

10. H. Gerischer, Faraday Discuss. Chem. Soc. 58 (1974) 219

11. A. Hagfeldt, M. Grätzel, Chem. Rev. 95 (1995) 49

12. M.K. Nazeeruddin, A. Kay, I. Rodicio, R. Humphry-Baker, E. Müller, P. Liska, N. Vlachopoulos, M. Grätzel, J.Am. Chem. Soc. 115 (1993) 6382

13. M. Grätzel, Prog. Photovolt. Res. Appl. 8 (2000) 171

14. M. Grätzel, Nature 414 (2001) 338

15. G. Boschloo, A. Hagfeldt, Acc. Chem. Res. 42 (2009) 1819

16. A.J. Frank, N. Kopidakis, J. Van de Lagemaat, Coord. Chem. Rev. 248 (2004) 1165

17. P.J. Cameron, L.M. Peter, S.M. Zakeeruddin, M. Grätzel, Coord. Chem. Rev. 248 (2004) 1447

18. A. Nattestad, M. Ferguson, R. Kerr, Y.B. Cheng, U. Bach, Nanotechnology 19 (2008) 295304

19. X. Chen, S.S. Mao, Chem. Rev. 2007, 107, 2891

20. H. Rensmo, K. Keis, H. Lindström, S. Södergren, A. Solbrand, A. Hagfeldt, S.E. Lindquist, J. Phys. Chem. B 101 (1997) 2598

21. I. Venditti, N. Barbero, M.V. Russo, A. Di Carlo, F. Decker, I. Fratoddi, C. Barolo, D. Dini, Mater. Res. Expr. 1 (2014) 015040

22. F. Odobel, Y. Pellegrin, E.A. Gibson, A. Hagfeldt, A.L. Smeigh, L. Hammarström, Coord. Chem. Rev. 256 (2012) 2414

23. J. He, H. Lindström, A. Hagfeldt, S.E. Lindquist, Solar En. Mater. Solar Cells 62 (2000) 265

24. A. Nattestad, A.J. Mozer, M.K.R. Fischer, Y.B. Cheng, A. Mishra, P. Bäuerle, U. Bach, Nature Mater. 9 (2010) 31

25. L. Li, E.A. Gibson, P. Qin, G. Boschloo, M. Gorlov, A. Hagfeldt, L. Sun, Adv. Mater. 22 (2010) 1759

26. E.A. Gibson, M. Awais, D. Dini, D.P. Dowling, M.T. Pryce, J.G. Vos, G. Boschloo, A. Hagfeldt, Phys. Chem. Chem. Phys. 15 (2013) 2411

27. P. Qin, M. Linder, T. Brinck, G. Boschloo, A. Hagfeldt, L. Sun, Adv. Mater. 21 (2009) 2993

28. P. Qin, H. Zhu, T. Edvinsson, G. Boschloo, A. Hagfeldt, L. Sun, J. Am. Chem. Soc. 130 (2008) 8570

29. A. Nattestad, M. Ferguson, R. Kerr, Y.B. Cheng, U. Bach, Nanotechnology 19 (2008) 295

30. S. Ito, P. Chen, P. Comte, M.K. Nazeeruddin, P. Liska, P. Pechy, M. Grätzel, Progr. Photovolt. Res. Appl. 15 (2007) 603

31. J. He, H. Lindström, A. Hagfeldt, S.E. Lindquist, J. Phys. Chem. B 103 (1999) 8940

32. S. Sumikura, S. Mori, S. Shimizu, H. Usami, E. Suzuki, J. Photochem. Photobiol. A 199 (2008) 1

33. S. Powar, Q. Wu, M. Weidelener, A. Nattestad, Z. Hu, A. Mishra, P. Bauerle, L. Spiccia, Y.B. Cheng, U. Bach, Energy Environ. Sci. 5 (2012) 8896

34. S. Ito, T.N. Murakami, P. Comte, P. Liska, C. Grätzel, M.K. Nazeeruddin, M. Grätzel, Thin Solid Films 516 (2008) 4613

35. X.L. Zhang, F. Huang, A. Nattestad, K. Wang, D. Fu, A. Mishra, P. Bäuerle, U. Bach, Y.B. Cheng, Chem. Commun. 47 (2011) 4808

36. X.L. Zhang, Z. Zhang, D. Chen, P. Bauerle, U. Bach, Y.B. Cheng, Chem. Commun. 48 (2012) 9885

37. M. Awais, M. Rahman, J.M. Don MacElroy, D. Dini, J.G. Vos, D.P. Dowling, Surf. Coat. Techn. 205 (2011) S245

38. Y. Shi, R.B.M. Hill, J.H. Yum, A. Dualeh, S. Barlow, M. Grätzel, S.R. Marder, M.K. Nazeeruddin, Angew. Chem. Int. Ed. 50 (2011) 6619

39. V. Novelli, M. Awais, D.P. Dowling, D. Dini, Am. J. Anal. Chem. 6 (2015) 176

40. S. Sheehan, G. Naponiello, F. Odobel, D.P. Dowling, A. Di Carlo, D. Dini, J. Solid State Electrochem. 19 (2015) 975

41. C.H. Chang, Y.C. Chen, C.Y. Hsu, H.H. Chou, J.T. Lin, Org. Lett. 14 (2012) 4726

42. J. Warnan, J. Gardner, L. Le Pleux, J. Petersson, Y. Pellegrin, E. Blart, L. Hammarström, F. Odobel, J. Phys. Chem. C 118 (2014) 103

43. G.C. Vougioukalakis, A.I. Philippopoulos,T. Stergiopoulos, P. Falaras, Coord. Chem. Rev. 255 (2011) 2602

44. R.K. Kanaparthi, J. Kandhadi, L.G. Giribabu, Tetrahedron 68 (2012) 8383

45. J. Park, C. Barolo, F. Sauvage, N. Barbero, C. Benzi, P. Quagliotto, S. Coluccia, D. Di Censo, M. Grätzel, M.K. Nazeeruddin, G. Viscardi, Chem. Commun. 48 (2012) 2782

46. J. Park, N. Barbero, J. Yoon, E. Dell'Orto, S. Galliano, R. Borrelli, J.H. Yum, D. Di Censo, M. Grätzel, M. K. Nazeeruddin, C. Barolo, G. Viscardi, Phys. Chem. Chem. Phys. 16 (2014) 24173

47. C. Magistris, S. Martiniani, N. Barbero, J. Park, C. Benzi, A. Anderson, C. Law, C. Barolo, B. O'Regan, Renew. Energy 60 (2013) 672

48. M. Awais, E.Gibson, J.G. Vos, D.P. Dowling, A. Hagfeldt, D. Dini, ChemElectroChem 1 (2014) 384

49. F. De Rossi, L. Di Gaspare, A. Reale, A. Di Carlo, T.M. Brown, J. Mater. Chem. A 1 (2013) 12941

50. A.G. Marrani, V. Novelli, S. Sheehan, D.P. Dowling, D. Dini, ACS Appl. Mater. Interfaces 6 (2014) 143

51. G. Boschloo, A. Hagfeldt, J. Phys. Chem. B 105 (2001) 3039

52. R. Schöllhorn, Physica B 99 (1980) 89

53. M. Awais, D.P. Dowling, M. Rahman, J.G. Vos, F. Decker, D. Dini, J. Appl. Electrochem. 43 (2013) 191

54. M. Awais, D. Dini, J.M. Don MacElroy, Y. Halpin, J.G. Vos, D.P. Dowling, J. Electroanal. Chem. 689 (2013) 185

55. G. Boschloo, H. Lindström, E. Magnusson, A. Holmberg, A. Hagfeldt, J. Photochem. Photobio. A 148 (2002) 11